33rd Annual International Conference of the IEEE EMBS
Boston, Massachusetts USA, August 30 - September 3, 2011

Effect of Self-Gating on Action Potential Firing at Neuromuscular Junction

M. Mostafizur Rahman, Mufti Mahmud, *Graduate student member,* IEEE, and Stefano Vassanelli

***Abstract*—The neuromuscular junction (NMJ) is the place where the axon terminal of motoneuron connects the 'endplate' of a muscle fiber. During this transduction a large depolarization (endplate potential) caused by the nerve impulse opens a large number of voltage-sensitive sodium channels at the post-junctional terminal. As a result, action potentials are generated and propagated along the muscle fiber causing contraction. This work shows simulated results of the voltage-dependent sodium channels' firing behavior at the NMJ using a mathematical model. It is found that the firing behavior of the sodium channels change basing on their activation and inactivation kinetics which are highly influenced by the self-gating behavior of the sodium conductances. The simulation results showed that self-gating of sodium channels increase conduction efficiency at the NMJ and decrease threshold for firing.**

Keywords— Self-gating; voltage-dependent sodium channels; neuromuscular junction; action potentials.

I. Introduction

THE Neuromuscular Junction (NMJ) is a structure that fosters and ensures a quick and efficient transmission of an action potential into the postsynaptic target area, i.e., the muscle, causing a contraction [1]. At the presynaptic end, the motor axon ends near the surface of the muscle fiber and divides into a number of short processes that lie embedded in grooves on the muscle-fiber surface, also known as motor endplate. The pulse carried by the presynaptic neuron when reaches the synapse causes release of Acetylcholine (ACh, the neurotransmitter at the synapse) to the postsynaptic membrane, i.e., the muscle fiber membrane. This depolarizes the postsynaptic membrane causing an increase in the membrane potential, eventually triggering the action potential. The mechanism of neurotransmitter conduction at the NMJ has been extensively studied by many researchers [2], [3].

The extracellular potential in the narrow extracellular space between nerve cell and muscular fiber (cleft) is affected by the current flow generated by the opening of sodium channels; consequently, voltage-dependent processes may be affected in the adjacent membranes. According to this hypothesis, the voltage drop in the cleft may modify the voltages across the muscle fiber membrane, thus increasing the probability of opening the voltage-gated ion channels. This phenomenon of current passing through weakly opened sodium channels and decreasing the potential of the extracellular space by a positive feedback was previously described in a general cell-to-substrate adhesion contact and termed "self-gating" [4]. During the presynaptic pulse's efficient transmission, the self-gating behavior of voltage-gated sodium channels plays an important role [4].

Considering critical parameters like cleft dimensions, axon terminal button radius, junction potential, and channel density the behavior of action potential firing may be changed. This behavioral change is hypothesized to be mainly due to the sudden transitions between states of low and high membrane conductance. To this hypothesis, in this work, we investigated the effects of self-gating on firing behavior through activation, inactivation, and gating kinetics of sodium channels at the rat NMJ and show that the change in firing behavior is indeed caused by the transitions during the self-gating of channels within the postsynaptic membrane. Also, the self-gating causes a drop in the action potential firing threshold compared to the non-self-gating situation.

II. The Model and Its Parameters

To model the rat NMJ (figure 1), we considered a 50 μm diameter and 500 μm long barrel shaped muscle fiber. To form a synapse, the circular shape axon terminal of 10 μm radius (a_j) [5] is connected to the highly-excitable region of muscle fiber membrane (7.85×10^{-8} m^2). The sodium channels density in the endplate was 3700 channels/μm^2 [6] and maximum conductance γ_{jm} of voltage-gated sodium channels was 9 pS / channel [7]. The global sodium conductance ($Glob_{gjm}$) is the total sodium conductance of the endplate motoneuron (eq. 3). The potential at the

Manuscript received April 15, 2011.

M. Mostafizur Rahman is with the NeuroChip Laboratory of Department of Human Anatomy & Physiology and Department of Information Engineering, University of Padova, 35131, Padova, Italy (e-mail: rahman@dei.unipd.it)

Mufti Mahmud is with the NeuroChip Laboratory of Department of Human Anatomy & Physiology, University of Padova, 35131, Padova, Italy (e-mail: mahmud@dei.unipd.it)

Stefano Vassanelli is with the NeuroChip Laboratory of Department of Human Anatomy & Physiology, University of Padova, 35131, Padova, Italy. (Corresponding Author; phone: +39 049 8275337; fax: +39 049 8275331; e-mail: stefano.vassannelli@unipd.it)

neuromuscular junction (V_j) is calculated using eq. 4 from the $Glob_{gjm}$ and other contributors, such as V_j itself, the sodium-specific reversal potential V_0 (50 mV) [7], the global resistance of the cleft (R_j), the intracellular potential (V_m) (figure 2). The cleft distance (d_j, 50 nm [5]), the electrolyte resistivity (ρ_j, 100 Ω [4]) are used in calculating the R_j. The endplate sodium current (EPI_{Na}) is calculated using $Glob_{gjm}$ and V_j by eq. 1.

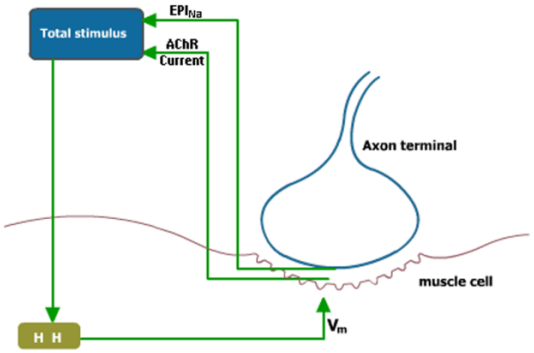

Fig. 1. The NMJ model diagram. The total stimulus current to calculate the membrane potential (V_m) at the muscle is derived by integrating the sodium current (EPI_{Na}) generated at the motoneuron endplate and the AChR current at the cleft. This V_m is fed back to the cleft to calculate the V_j and the other entities. HH denotes Hodgkin-Huxley formalism.

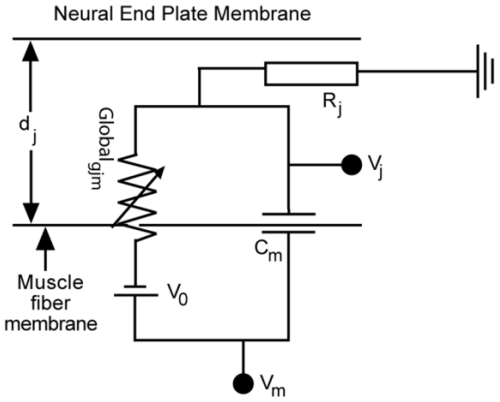

Fig. 2. Circuit diagram of the NMJ model.

$$\mathrm{EPI_{Na}} = \mathrm{Glob_{gjm}}.(V_m - \mathrm{V_j} - \mathrm{E_{Na}}) \quad (1)$$

where

$$\mathrm{g_{jm}} = \bar{\mathrm{g}}_{\mathrm{jm}}.\mathrm{m}^3.\mathrm{h} \quad (2)$$

$$\mathrm{Glob_{gjm}} = \mathrm{g_{jm}} \cdot \pi \mathrm{a_j}^2 \quad (3)$$

$$R_j = \frac{\rho_j}{5\pi d_j}$$

$$\mathrm{V_{j+1}} = \mathrm{Globgjm} \times \mathrm{R_j} \frac{\mathrm{V_m}-\mathrm{V_j}-\mathrm{V_0}}{1+(\mathrm{R_j}\cdot\mathrm{Globgjm})} \quad (4)$$

At the rat NMJ transitions between permissive and non-permissive states of the ion channels are assumed to obey first-order kinetics of the Hodgkin-Huxley formalism [8].

$$\alpha_m = \frac{0.14(V_m+63.5)}{1-exp\,(-(V_m+63.5)/6.8)}$$

$$\beta_m = 0.5\ exp(\frac{-V_m}{27})$$

$$\frac{dm}{dt} = \alpha_\mathrm{m}(1-\mathrm{m}) - \beta_\mathrm{m}\mathrm{m}$$

$$\alpha_h = 0.1\ exp(\frac{-(V_m+40)}{20})$$

$$\beta_h = \frac{1}{1+exp\,(-(V_m+46)/10)}$$

$$\frac{dh}{dt} = \alpha_h(1-h) - \beta_h h$$

$$\alpha_n = \frac{0.006(V_m+41.6)}{1-exp\,(-(V_m+41.6)/4)}$$

$$\beta_n = 0.037\ exp(\frac{-(V_m+41.6)}{35.3})$$

$$\frac{dn}{dt} = \alpha_n(1-n) - \beta_n n$$

with,

$$I_{Na} = \overline{g_{Na}}\,.m^3.h.(V_m - E_{Na})$$

$$I_K = \overline{\mathrm{g_K}}.n.(V_m - E_K)$$

$$I_L = \overline{\mathrm{g_L}} * (V_m - V_L)$$

and

$$V_m = 1/C_m \cdot (I_{Na} + I_K + I_L + I_{stim}) \quad (5)$$

Where $\overline{g_{Na}}$ (45 mS/cm^2, [9]), $\overline{\mathrm{g_K}}$ (29.9 mS/cm^2, [10]), and $\overline{\mathrm{g_L}}$ (1 mS/cm^2) are the maximum conductances for sodium, potassium, and leakage, respectively. E_{Na} (45 mV, [9]), E_K (-73 mV, [10]), E_L (-90 mV, [9]) are the Nernst equilibrium potentials for sodium, potassium, and leakage, respectively. C_m is the membrane capacitance (4 µF, [9]). I_{stim} is the total stimulus current calculated using eq. 7.

The AChR current (eq. 6), generated in the cleft is modeled as a double exponential function with a decay and a rise time constant, τ_d (0.564 ms) and τ_r (0.162 ms) [11].

$$\mathrm{AChRCurrent} = \mathrm{C_j}.\mathrm{V_m}.\left(\exp\left(-\frac{\mathrm{t}}{\tau_\mathrm{d}}\right) - \exp\left(-\frac{\mathrm{t}}{\tau_\mathrm{r}}\right)\right) \quad (6)$$

where C_j is the total ACh receptor (AChR) conductance at the cleft which can be calculated as a product of maximum AChR conductance per channel (59.1 pS / channel, [12]), number of active AChR, and the area of the cleft ($\pi \cdot a_j^2$). Literature suggests that the total number of AChR in the cleft is about (10000 AChR channels / µm^2) out of which 3% channels are considered to be open at a time of synaptic activation [6].

As seen in figure 1, the AChR current together with the EPI_{Na} act as stimulus current to the Hodgkin-Huxley based V_m (as in eq. 5) calculation at the muscle fiber.

$$I_{stim} = \mathrm{AChRCurrent} + \mathrm{EPI_{Na}} \quad (7)$$

III. Simulation Results

Simulation of the rat NMJ was done in MATLAB (version: 7.9.0.529, R2009b; http://www.mathworks.com) environment through scripting.

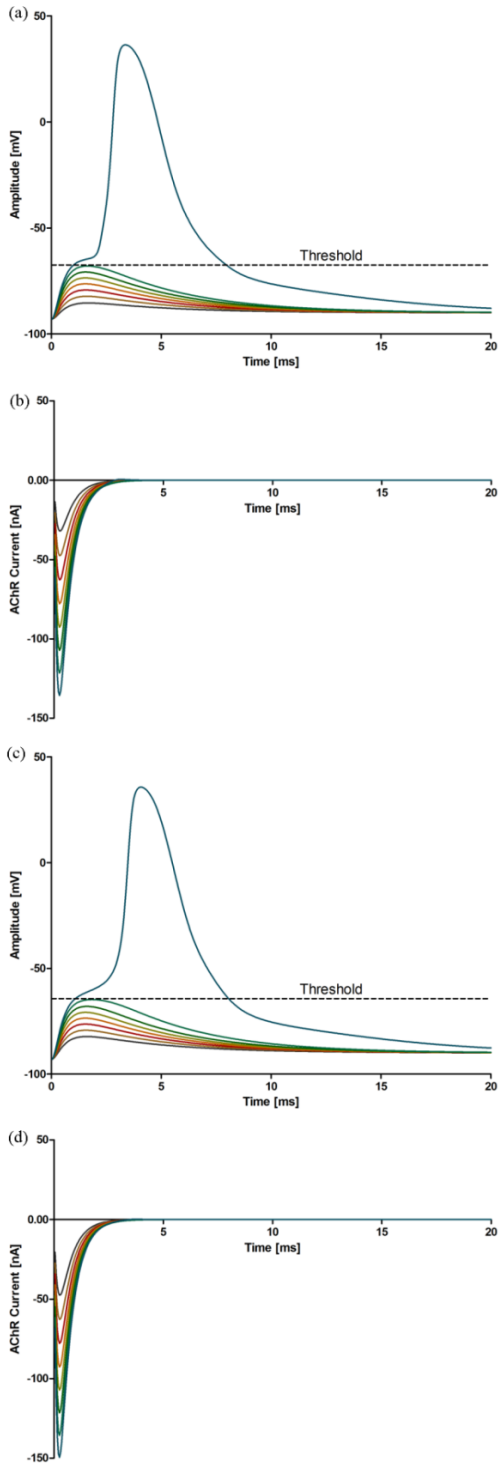

Fig. 3. (a) Threshold of muscle fiber action potential under self-gating condition. (b) AChR current under self-gating condition. (c) Threshold of muscle fiber action potential under non-self-gating condition. (d) AChR current under non-self-gating condition. The membrane potential and the AChR current are colorwise grouped.

Figure 3(a) is showing a threshold potential for firing of -68 mV and figure 3(b) the corresponding ACh dependent synaptic current under self-gating condition. However, under non-self-gating condition a slight higher threshold potential of -64.75 mV was noticed (figure 3(c)), which was reflected also in the higher amount of AChR current (figure 3(d)). It is worth mentioning that the threshold is a special potential where the process of depolarization becomes regenerative to establish a positive feedback which eventually causes an action potential. At threshold, depolarization opens more voltage-gated sodium channels letting sodium ions to flow into the cell, which in turn further depolarizes the cell and opens even more voltage-gated sodium channels. The threshold potential was determined from the peak of the maximum voltage that failed to trigger an action potential [13].

Moreover, when constant stimulus current was injected the NMJ model showed repetitive firing behavior. This was mainly due to the large stimulus current which made the potential to overshoot. Under self-gating state -135 nA of stimulus current was good enough to generate a train of action potentials; and under non-self-gating state that was found to be -137 nA. These amounts of stimulus currents can be compared to the maximum synaptic currents at which the cell triggers action potential (figure 3(b) and 3(d)). Figure 4 shows the effect of self-gating and non self-gating condition on repetitive firing at a constant stimulus of -150 nA instead of the ACh based sodium synaptic current. It is evident that during the self-gating the cell fires more action potentials than that of the non-self-gating condition.

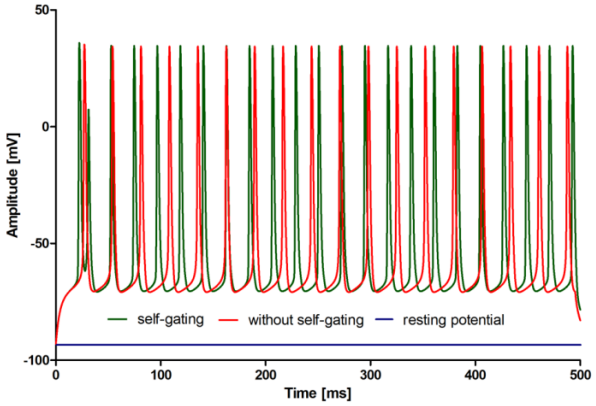

Fig 4. Repetitive firing behavior at rat NMJ. Action potentials were generated in response to a -150 nA constant current injection.

It is being found that the frequency of repetitive firing is dependent on the decay rate of the hyperpolarization phase, which in turn is dependent on the values of the individual ionic currents and their associated conductances. To show the change in frequency of action potential firing under self-

gating and non-self-gating conditions, action potentials were generated for 500 ms by applying stimulus ranging from -135 nA to -240 nA and they were counted and plotted in a semi-logarithm scale (figure 5). This figure shows a higher firing frequency at self-gating state, as expected.

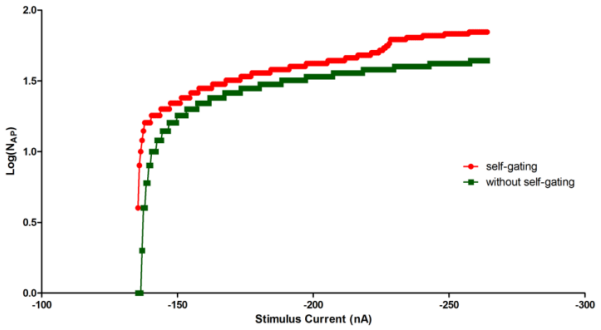

Fig 5. Semi-logarithmic plot of action potential firing frequency under self-gating and non-self-gating conditions.

IV. Discussion and Conclusion

In previous work we explored the conductance profiles of the NMJ under the self-gating and non-self-gating conditions. The conductance associated to voltage-gated sodium channels depends on the voltage drop of V_m–V_j across the membrane [4]. The V_j was calculated for different membrane potentials which showed that the voltage-dependent sodium conductance at the NMJ undergoes self-gating due to the drop of V_j in the synaptic cleft and in the following depolarization of the potential (V_m–V_j) across the membrane [14], [15].

Also, during the self-gating condition a switching behavior was noticed in the sodium channels conductance: from low to high during depolarization and from high to low during repolarization of membrane potential. At this time bistability and hysteresis of sodium channels occurred which explains the transmission efficiency of the NMJ under self-gating condition [14].

The same parameters were used in simulating the recovery period of sodium channels from inactivation which showed to be slightly higher recovery period under self-gating condition. During the activation of sodium channels at the muscle, a higher activation rate under self-gating condition was noticed using Hodgkin-Huxley formulation [15].

In conclusion, the behavioral difference in the firing of action potentials in the NMJ is mainly caused by a sudden transition in the opening of sodium channels during self-gating and gradual opening of sodium channels in non-self-gating conditions. Under self-gating, the channels remain open for a longer period letting inward currents to flow during repolarization. This sustained current flow is likely favoring cell depolarization and action potential firing in the muscle.

Under self-gating condition the threshold potential at the NMJ is lower than that of non-self-gating condition. The higher number of sodium channels' opening during the self-gating condition causing the increase of sodium current intensity during the first phase of action potential which directly affects the depolarization of the cell, thus, making it fire at a lower firing threshold.

And as well the action potential firing frequency is higher at the self-gating state. The muscle unit's firing rate increases under self-gating condition due to the fact that the longer inactivation time is compensated by the switching behavior of the sodium current. This allows fast and larger entrance of sodium current in every successive spike.

References

[1] W. Hoch, "Formation of the neuromuscular junction," *Eur. J. Biochem.*, Vol. 265, pp. 1-10, 1999.

[2] J. R. Sanes, J. W. Lichtman, "Development of the Vertebrate Neuromuscular Junction," *Annual Review of Neuroscience*, Vol. 22, pp. 389-442, 1999.

[3] X. Guo, M. Das, J. Rumsey, M. Gonzalez, M.Stancescu, J. Hickman, "Neuromuscular junction formation between human stem-cell-derived motoneurons and rat skeletal muscle in a defined system," *Tissue Eng Part C Methods*, Vol. 16, No. 6, pp. 1347-55, 2010.

[4] P. Fromherz, "Self-Gating of Ion Channels in Cell Adhesion," *Phys. Rev. Lett.*, Vol. 78, No. 21, pp. 4131--4134, 1997.

[5] S. J. Wood, C. R. Slater, "Safety Factor at the Neuromuscular Junction," *Prog. Neurobiol.*, Vol. 64, No. 4, pp. 393-429, 2001.

[6] J.L. Boudier, T. LeTreut, E. Jover, "Autoradiographic localization of voltage-dependent sodium channels on the mouse neuromuscular junction using 125 alpha scorpion toxin. II. Sodium channel distribution on postsynaptic membranes," *J. Neurosci.*, Vol. 12, No. 2, pp. 454-466, 1992.

[7] J. F. Desaphy, A. De Luca, P. Imbrici, D.C. Camerino, "Modification by Ageing of the Tetrodotoxin-Sensitive Sodium Channels in Rat Skeletal Muscle Fibres," *Biochim Biophys Acta.*, Vol. 1373, No. 1, pp. 37-46, 1998.

[8] A. L. Hodgkin, A. F. Huxley,, "A Quantitative Description of Membrane Current and its Application to Conduction and Excitation in Nerve," *J. Physiol.*, Vol. 117, pp. 500-544, 1952.

[9] P. A. Pappone, "Voltage clamp experiments in normal and denervated mammalian skeletal muscle fibers," *J. Physiol.*, Vol. 306, pp. 377-410, 1980.

[10] S. Hollingworth, M. W. Marshall, E. Robson, "Ionic currents and charge movements in organ-cultured rat skeletal muscle", *J. Physiol.*, Vol. 357, pp. 369-386, 1984.

[11] S.D. Head, "Temperature and endplate currents in rat diaphragm," *J. Physiol.*, Vol. 334, pp. 441-459, 1983.

[12] A. Villarroel, B. Sakmann, "Calcium permeability increase of endplate channels in rat muscle during postnatal development," *J. Physiol.*, Vol. 496, No. 2, pp. 331-338, 1996.

[13] S.J. Wood, C.R. Slatar, "Action potential generation in rat fast and slow-twitch muscles," *J. physiol.*, Vol. 486, No.2, pp. 401-410, 1995.

[14] M. M. Rahman, M. Mahmud, S. Vassanelli, "Self-Gating of sodium channels at neuromuscular junction", In: *Proc. of the 5th IEEE EMBC Conference on Neural Engineering (NER2011)*, Cancun, Mexico, 2011, pp. 208-211.

[15] M. M. Rahman, M. Mahmud, S. Vassanelli, "Sodium channels' kinetics under self-gating condition at neuromuscular junction," Manuscript under preparation.